Click Chemistry-mediated Biotinylation Reveals a Function for the Protease BACE1 in Modulating the Neuronal Surface Glycoproteome*[S]

Julia Herber‡§‖‖, Jasenka Njavro‡§‖‖, Regina Feederle‡¶‖, Ute Schepers**, Ulrike C. Müller‡‡, Stefan Bräse**, Stephan A. Müller‡§, and Stefan F. Lichtenthaler‡§¶§§¶¶

The cell surface proteome is dynamic and has fundamental roles in cell signaling. Many surface membrane proteins are proteolytically released into a cell's secretome, where they can have additional functions in cell-cell-communication. Yet, it remains challenging to determine the surface proteome and to compare it to the cell secretome, under serum-containing cell culture conditions. Here, we set up and evaluated the 'surface-spanning protein enrichment with click sugars' (SUSPECS) method for cell surface membrane glycoprotein biotinylation, enrichment and label-free quantitative mass spectrometry. SUSPECS is based on click chemistry-mediated labeling of glycoproteins, is compatible with labeling of living cells and can be combined with secretome analyses in the same experiment. Immunofluorescence-based confocal microscopy demonstrated that SUSPECS selectively labeled cell surface proteins. Nearly 700 transmembrane glycoproteins were consistently identified at the surface of primary neurons. To demonstrate the utility of SUSPECS, we applied it to the protease BACE1, which is a key drug target in Alzheimer's disease. Pharmacological BACE1-inhibition selectively remodeled the neuronal surface glycoproteome, resulting in up to 7-fold increased abundance of the BACE1 substrates APP, APLP1, SEZ6, SEZ6L, CNTN2, and CHL1, whereas other substrates were not or only mildly affected. Interestingly, protein changes at the cell surface only partly correlated with changes in the secretome. Several altered proteins were validated by immunoblots in neurons and mouse brains. Apparent nonsubstrates, such as TSPAN6, were also increased, indicating that BACE1-inhibition may lead to unexpected secondary effects. In summary, SUSPECS is broadly useful for determination of the surface glycoproteome and its correlation with the secretome. ***Molecular & Cellular Proteomics 17: 1487–1501, 2018. DOI: 10.1074/mcp.RA118.000608.***

Cell surface membrane proteins are essential for the communication between cells and their environment. They have fundamental roles in physiology and pathophysiology and represent major protein targets for existing drugs and drug development (1). The cell surface proteome is dynamic, which allows cells to regulate the levels and functions of its surface membrane proteins, for example in cell adhesion and signal transduction. Removal of membrane proteins from the surface may occur through endocytosis or proteolysis, where proteases in the membrane or the extracellular space, such as a disintegrin and metalloprotease 10 and 17 (ADAM10, ADAM17) and β-site APP cleaving enzyme 1 (BACE1)[1], cleave off a membrane protein's ectodomain (2–4). This proteolytic process is referred to as ectodomain shedding and does not only affect the surface proteome, but also a cell's secretome, which comprises both soluble, secreted proteins and shed membrane protein ectodomains. The latter may be active biomolecules, such as growth factors (*e.g.* TGFα) and cytokines (*e.g.* TNFα) but may also act as decoy receptors for their membrane-bound counterparts (5). Therefore, it is important to investigate how changes in the surface proteome are linked to alterations in the secretome during (patho)physiological conditions. But despite the tight coupling of a cell's surface proteome and secretome, it remains challenging to directly analyze both in the presence of serum proteins within the same experiment.

From the ‡German Center for Neurodegenerative Diseases (DZNE), Munich, Germany; §Neuroproteomics, School of Medicine, Klinikum rechts der Isar, Technische Universität München, Munich, Germany; ¶Munich Cluster for Systems Neurology (SyNergy), Munich, Germany; ‖Institute for Diabetes and Obesity, Monoclonal Antibody Research Group, Helmholtz Zentrum München, German Research Center for Environmental Health (GmbH), Munich, Germany; **Karlsruhe Institute of Technology (KIT), Institute of Toxicology and Genetics (ITG), Karlsruhe, Germany; ‡‡Department of Functional Genomics, Institute for Pharmacy and Molecular Biotechnology, Heidelberg University Heidelberg, Germany; §§Institute for Advanced Study, Technische Universität München, Munich, Germany

Received January 22, 2018, and in revised form, April 16, 2018
Published, MCP Papers in Press, April 30, 2018, DOI 10.1074/mcp.RA118.000608

Determination of the cell surface membrane proteome by mass spectrometry-based proteomics critically depends on the purity of surface membrane protein preparations. Besides subcellular fractionation and surface protein shaving, the biotinylation of cell surface proteins has become popular (6). However, biotinylation of lysine side chains in surface proteins has the drawback to block subsequent tryptic digestion during sample preparation. More recent approaches, such as cell surface capturing (CSC) and periodate oxidation and aniline-catalyzed oxime ligation (PAL), circumvented this issue by exploiting the fact that most surface membrane proteins are glycosylated or predicted to be glycosylated (7, 8). CSC and PAL use a two-step chemical protocol, which involves oxidation of protein glycans to aldehydes and subsequent labeling with a biotin-containing tag for further glycoprotein enrichment. The sugar oxidation is performed on living cells, which facilitates the selective enrichment of cell surface, but not intracellular glycoproteins. Despite their suitability for surface protein analysis, CSC and PAL are not well suited for proteomic analysis of the corresponding cell secretome as cells are mostly cultured in the presence of serum or serum-like supplements, which contain high concentrations of glycoproteins, in particular immunoglobulins. Those serum-derived glycoproteins would also be labeled, but—because of their high abundance—prevent efficient detection of the low-abundant cellular secretome proteins. Thus, alternative methods for secretome analysis such as SPECS (secretome protein enrichment with click sugars) have been developed (9). SPECS metabolically labels only newly synthesized cellular glycoproteins with click chemistry-suitable sugars (9–12). Subsequently, click chemistry allows selective enrichment of the glycoproteins from the serum protein-containing conditioned medium. A similar approach was developed where proteins are labeled with nonnatural amino acids amenable to click chemistry-mediated labeling (13). SPECS has previously been used to enrich cellular glycoproteins (11) but was not able to distinguish between surface and intracellular proteins.

Here, we set up a method for specific labeling and relative quantification of cell surface membrane glycoproteins, which only requires a single chemical reaction and is complementary to secretome analyses using the SPECS method in the same experiment. The new method is named **SU**rface-**S**panning **P**rotein **E**nrichment with **C**lick **S**ugars (SUSPECS).

[1] The abbreviations used are: BACE1, β-site APP cleaving enzyme 1; ADAM10/17, A disintegrin and metalloprotease 10/17; CSC, cell surface capturing; DBCO, Dibenzylcyclooctyne; DEA, diethyl amine; DIV, Day in vitro; DTAF, Dichlorotriazinylamino fluorescein; FDR, False discovery rate; GPI, Glycosylphosphatidylinositol; IAA, Iodoacetamide; IB, Immunoblot; KO, Knockout; LFQ, Label free quantification; Ac_4-ManNAz, tetra-acetylated N-azidomannosamine; NHS, N-Hydroxysuccinimide; PAL, periodate oxidation and aniline-catalyzed oxime ligation; PDL, Poly-D-lysine; QARIP, quantitative analysis of regulated intramembrane proteolysis; RT, Room temperature; TGN, Trans-Golgi network; TM, Transmembrane (type); w/v, Weight per volume.

Our new approach identified nearly 700 transmembrane glycoproteins at the surface of primary murine neurons using label-free quantitative proteomics. To demonstrate the utility of SUSPECS, we applied it to study the protease BACE1, which is a key drug target in Alzheimer's disease, as it cleaves the membrane protein APP to generate the pathogenic amyloid β peptide (14). Yet, BACE1 also cleaves numerous other membrane protein substrates (9, 15–19), whose functions may be affected when BACE1 is therapeutically blocked. In fact, BACE1-deficient mice show several defects and phenotypes (20). Therefore, we investigated the neuronal surface proteome after pharmacological inhibition of BACE1 and compared the results to changes in the secretome.

EXPERIMENTAL PROCEDURES

MATERIALS

The following antibodies were used: polyclonal DNER (R&D Systems, AF2254), monoclonal SEZ6 clone 14E5 (19) and SEZ6L (R&D Systems, MN; AF4804), SEZ6L2 (R&D Systems, AF4916), monoclonal BACE1 clone 3D5 (kindly provided by Robert Vassar), polyclonal TSPAN6 (Abgent, CA; AP9224b), monoclonal MMP17 clone EP1270Y (Abcam, Cambridge, UK; ab51075), monoclonal Golgin-97 (Invitrogen, CA; A21270), monoclonal NEO1 clone 21A8 (11), polyclonal RGMa (R&D Systems, AF2458), monoclonal GluR2 (MAB397, Millipore, Merck, Darmstadt, Germany), polyclonal Calnexin (Enzo, Stressgen, Farmingdale, NY, ADI-SPA-860), monoclonal β-actin clone AC-74 (Sigma, Merck; A5316), HRP coupled anti-mouse (Promega, Mannheim, Germany; W402B) and anti-rabbit secondary (Promega, W401B), HRP-coupled anti-goat (Santa Cruz, sc-2020), anti-rat (Santa Cruz, TX; sc-2006) and anti-sheep (Santa Cruz, sc-2473). Monoclonal APLP1 clone 8G6 (mouse IgG2a/k) was generated by peptide immunization (AA75-EPDPQRSRRCLLDPQR-AA90 within APLP1 copper binding domain) of C57BL/6 mice using standard procedures (21).

The following reagents and media were used: DMEM, Neurobasal medium, HBSS, and B27 (Thermo Fisher Scientific, Darmstadt, Germany), protease inhibitor (Sigma, P8340), C3 (β-secretase inhibitor IV; Calbiochem, 565788, final concentration 2 μM), tetra-acetylated N-azidoacetylmannosamine (Ac_4-ManNAz), Dichlorotriazinylamino fluorescein DTAF-conjugated Streptavidin (Dianova, Hamburg, Germany), Sulfo-dibenzylcyclooctyne-biotin (Sulfo-DBCO-Biotin, Jena Bioscience, Jena, Germany).

Immunofluorescence—COS-7 cells were cultured in DMEM supplemented with 10% fetal calf serum (FCS) and 1% Penicillin-Streptomycin (Pen/Strep). For immunofluorescent labeling of cell surface proteins, COS-7 cells were seeded onto poly-D-lysine (PDL)-coated glass coverslips in culture medium supplemented with 50 μM tetra-acetylated N-azidomannosamine (Ac_4-ManNAz) and cultured for 48h. Unfixed cells were washed twice with 1x phosphate buffered saline (PBS)

and metabolically labeled glycoproteins were biotinylated with 100 μM sulfo-DBCO-Biotin for 2 h at 4 °C. Subsequently, cells were fixed with 4% paraformaldehyde (PFA) in 1× PBS for 10 min at room temperature (RT). Biotinylated proteins were labeled with 2 μg/ml streptavidin-dichlorotriazinylamino fluorescein (DTAF) for 1 h at room temperature and nuclei were stained with 4 μg/ml Hoechst 33342 for 30min at RT. Coverslips were mounted in FluorSave (Calbiochem, Merck) onto glass slides and imaged with confocal microscopy using a Leica TCS SP5 Confocal Laser Scanning Microscope (LSM) or Zeiss LSM 510 Axio Observer. Pictures were processed with ImageJ (Fiji), Photoshop (Adobe) or ZEN2 (Zeiss).

Primary Cell Culture—Primary cortical neurons were extracted from wildtype C57BL/6 mouse embryos on embryonic day 16.5 like described before (22). Briefly, embryonic cortices were dissected and cleaned from meninges. Cortices were pooled and digested with 200 U papain (in DMEM-high glucose supplemented with L-cysteine, pH 7.4) at 37 °C for 15 min. Using a pipette, tissue was mechanically dissociated to obtain a single-cell-suspension. Cells were plated in PDL-coated T-175 cm flasks (20×10^6 cells for proteomic experiments) or on 6 cm dishes (4×10^6 cells for immunoblots (IB)) in plating medium (DMEM-high glucose, 10% FCS) and medium was changed after 3–4 h to culture medium (Neurobasal, 500 μM L-glutamine, 1% Penicillin/Streptomycin, 1× B27 supplement).

Treatment of Cells and Labeling of Surface Proteins—For metabolic labeling of newly synthesized glycoproteins, primary cortical neurons at 5 days *in vitro* (DIV) were cultured for 48 h in neuronal culture medium supplemented with 50 μM Ac_4-ManNAz and the BACE inhibitor C3 or dimethyl sulfoxide (DMSO) as control. 40×10^6 (for MS) and 4×10^6 (for IB) neurons were used per condition for proteomic and biochemical analysis, respectively. At DIV 7 cells were washed twice with 1x PBS (GIBCO). Biotinylation was performed via bioorthogonal click chemistry applying 100 μM sulfo-DBCO-Biotin and incubating 2 h at 4 °C. To remove sulfo-DBCO-Biotin in excess, cells were washed twice with 1× PBS and lysed in STET-lysis buffer (150 mM NaCl, 50 mM Tris (pH 7.5), 2 mM EDTA, 1% Triton X-100) with protease inhibitor. Lysates were cleared by centrifugation for 5 min at maximum speed and filtered through a 0.45 μM syringe filter (Millipore).

For immunoblot analyses, cells were lysed in STET-lysis buffer with protease inhibitor or SDS buffer (50 mM Tris (pH 8), 150 mM NaCl, 2 mM EDTA, 1% SDS) with protease inhibitor. Lysates were cleared by centrifugation for 5min at maximum speed. Cleared SDS-lysates were diluted 1:1 with RIPA buffer (10 mM Tris pH 8, 150 mM NaCl, 2 mM EDTA, 1% Triton X-100, 0.1% SDS, 0.1% Sodium deoxycholate) and sonicated.

Sample Preparation for Mass Spectrometry—Cleared cell culture lysates of 6 control (DMSO) and 6 inhibitor treated (C3) cell samples were loaded on a polyprep chromatography column (Bio-Rad, Munich, Germany) containing 300 μl of high capacity streptavidin agarose beads (Thermofisher) and washed twice with 10 ml 2% SDS in PBS to remove nonspecifically bound proteins. The flow-through was reloaded to increase the yield of bound biotinylated proteins. Each column was washed twice with 10 ml 2% SDS in PBS. Streptavidin-beads were transferred into an Eppendorf tube in 2% SDS in PBS and liquid was removed completely with a Hamilton syringe. Beads were boiled 5 min at 95 °C in 150 μl Lämmli buffer supplemented with 8 M urea and 3 mM biotin to elute the proteins. Samples were separated with 10% SDS-polyacrylamide gel electrophoresis (PAGE) and stained with 0.025% (w/v) Coomassie Brilliant Blue in 10% acetic acid for 15 min with horizontal shaking. The gel was destained in 10% acetic acid (2 × 30 min, 1× overnight) with horizontal shaking.

In-gel Digestion and Peptide Purification—Each lane was cut into 14 horizontal slices (=14 fractions) at equal height and subjected to tryptic in-gel digestion (23). Briefly, proteins residing in the gel were denatured with 10 mM dithiothreitol (DTT) in 100 mM ammonium bicarbonate (ABC) and reduced with 55 mM iodoacetamide (IAA) in 100 mM ABC. Proteolytic digestion was performed at 37 °C overnight using 150 ng trypsin per fraction. Peptides were extracted with 40% acetonitrile (ACN) supplemented with 0.1% formic acid, dried by vacuum centrifugation, and reconstituted in 0.1% formic acid for proteomic analysis.

LC-MS/MS Analysis—Each gel fraction was analyzed on an Easy nLC-1000 (Thermo Proxeon), which was coupled online via a nano electrospray source (Thermo Proxeon) to a Velos Pro Orbitrap Mass Spectrometer (Thermo). Peptides were separated on a self-packed C18 column (300 mm × 75 μm, ReproSil-Pur 120 C18-AQ, 1.9 μm, Dr. Maisch) with a binary gradient of water (A) and acetonitrile (B) containing 0.1% formic acid (0 min, 2% B; 3:30 min 5% B; 48:30 min, 25% B; 59:30, 35% B; 64:30, 60% B). Full MS spectra were acquired at a resolution of 70,000. The ten most intense peptide ions per spectrum were chosen for collision-induced dissociation (CID) within the ion trap. A dynamic exclusion of 40 s was applied for CID acquisition.

LC-MS/MS Data Analysis and Statistical Evaluation—Database search and label free quantification was performed with the software MaxQuant (version 1.5.5.1, maxquant.org). Trypsin was defined as protease (cleavage specificity: C-terminal of K and R). Carbamidomethylation of cysteines was defined as fixed modification. Oxidation of methionines and acetylation of protein N termini were defined as variable modifications. Two missed cleavages were allowed for peptide identification. The first search option was enabled with a precursor mass tolerance and a fragment mass tolerance of 20 ppm. The mass tolerances for the main search were set to 4.5 and 20 ppm for precursor and fragment ion masses, respectively. The false discovery rate (FDR) for both peptides and proteins was adjusted to less than 1% using a target and decoy approach (concatenated forward/reverse database) including the reference mouse proteome (UniProt, download: June 8,

2016; 16,798 entries). Common contaminants such as bovine proteins of fetal calf serum and human keratins were excluded. Label-free quantification (LFQ) intensity values were used for relative quantification. At least two ratio counts of unique peptides were required for protein quantification. Proteins were considered as identified, if they were detected by at least 2 unique peptides in at least 3 out of the 12 samples (six samples each with or without C3). Proteins identified by only one unique peptide were excluded for further statistical analysis.

For relative quantification the LFQ intensity ratios of C3 and vehicle (DMSO) treated samples were calculated separately for each biological replicate ($n = 6$) to account for experimental variations of different neuronal cell preparation batches. At least three LFQ ratios of biological replicates were required for statistical analysis. All LFQ ratios were log2 transformed and a one-sample *t* test ($\mu_0 = 0$) was applied to check if the average log2 LFQ ratio is different from zero. The *p* value threshold was adjusted for false discovery rate (5%) by applying Benjamini-Hochberg correction criteria. Classification of identified proteins was done using UniProt keywords and subcellular locations as well as the PANTHER (protein annotation through evolutionary relationship) classification system (http://www.pantherdb.org/).

The mass spectrometry proteomics data have been deposited to the ProteomeXchange Consortium via the PRIDE (24) partner repository with the data set identifier PXD008619 (Project webpage: http://www.ebi.ac.uk/pride/archive/projects/).

Mouse Strains—The following mice were used: wild type (WT) C57BL/6NCrl (Charles River) and BACE1−/− (Jackson Laboratory, strain B6.129- Bace1tm1Pcw/J, BACE1 KO). Mice were maintained on a 12/12 h light-dark cycle with food and water *ad libitum*. All animal procedures were carried out in accordance with the European Communities Council Directive (86/609/EEC). The animal protocols were approved by the Ludwig-Maximilians-University Munich and the government of Upper Bavaria.

Brain Fractionation—Brain cortices were isolated from postnatal day 7 (P7) BACE1−/− mice and WT littermates and homogenized in diethyl-amine (DEA) buffer (50 mM NaCl, 2 mM EDTA, 0.2% diethylamine, 1:250 protease inhibitor). Homogenates were directly neutralized with 0.5 M Tris buffer pH 6.8 and centrifuged at 20,000 × *g* for 10 min. The supernatants containing the soluble proteins were ultracentrifuged at 30,000 × *g* and 4 °C to obtain cleared DEA-fractions. Pellets (resulting from the first centrifugation step) were washed with 1× PBS to remove soluble proteins and lysed afterward in SDS buffer (50 mM Tris (pH 8), 150 mM NaCl, 2 mM EDTA, 1% SDS) with protease inhibitor. Samples were diluted 1:1 in RIPA buffer (10 mM Tris pH 8, 150 mM NaCl, 2 mM EDTA, 1% Triton X-100, 0.1% SDS, 0.1% Sodium deoxycholate) and sonicated. Quantification of protein concentrations was done with a BCA assay (Uptima Interchim, Montlucon, France) and 10–20 μg of total protein was used for IB analysis.

Experimental Design and Statistical Rationale—For MS experiments, we analyzed 6 biological replicates in 6 independent experiments. Each biological replicate originated a separate neuronal preparation (6 C57BL/6 mice). Cortices of all embryos (~6–9 per mouse) were pooled during one extraction (so that all neurons in one experiment have the same 'background'). 80×10^6 neurons were used for one biological replicate: half was treated with the BACE1 inhibitor C3 and half was vehicle-treated with DMSO. C3 and DMSO samples from one experiment were separated on a SDS-PAGE and analyzed by LC-MS/MS and quantified with a label-free approach. For quantification, we only considered proteins present in both groups (C3 and DMSO) in at least 3 out of 6 experiments. Statistical testing was performed with a one-sample *t* test and corrected for multiple hypothesis testing according to Benjamini-Hochberg.

Immunoblots of neurons were performed with at least 3 different neuronal preparations (divided in up to 3 experiments per preparation), which yielded 6–11 independent experiments per protein with each one C3 and one DMSO-treated group. Each protein was checked by immunoblotting in neurons originating 3 different mice. Immunoblots of mouse cortices were performed with 6 biological replicates. One biological replicate equals one WT and one B1−/− animal. Immunoblot experiments were statistically tested by applying the Mann-Whitney-*U* test.

RESULTS

Selective Labeling of Plasma Membrane Proteins—Previously, we developed the "secretome protein enrichment with click sugars" (SPECS) method (9), which uses click chemistry to label and identify the cellular secretome—comprising both soluble proteins and proteolytically released membrane protein ectodomains—by mass spectrometry. To be able to compare secretome changes to alterations in the surface proteome using material from the same cellular experiment, we first set up a workflow referred to as '**Su**rface-**S**panning **P**rotein **E**nrichment with **C**lick **S**ugars' (SUSPECS), where SPECS-like labeling is used to assess the surface proteome of glycosylated membrane proteins (Fig. 1). SUSPECS exploits the fact that according to the UniProt-database most membrane proteins are glycosylated (supplemental Fig. S1). For example, more than 90% of single-pass type I transmembrane proteins, to which most substrates of BACE1 and other surface proteases belong (9, 16, 17), are glycosylated (supplemental Fig. S1).

To facilitate the enrichment of glycoproteins, glycans were labeled with tetra-acetylated N-azidomannosamine (Ac_4-ManNAz), a click chemistry-suitable azido-modified mannose derivative. When taken up by cells, Ac_4-ManNAz is modified to *N*-azido-sialic acid and metabolically incorporated into the terminal glycan structures of newly synthesized glycosylated proteins (25, 26). After 2 days of continuous metabolic labeling, the conditioned medium was removed, and living cells

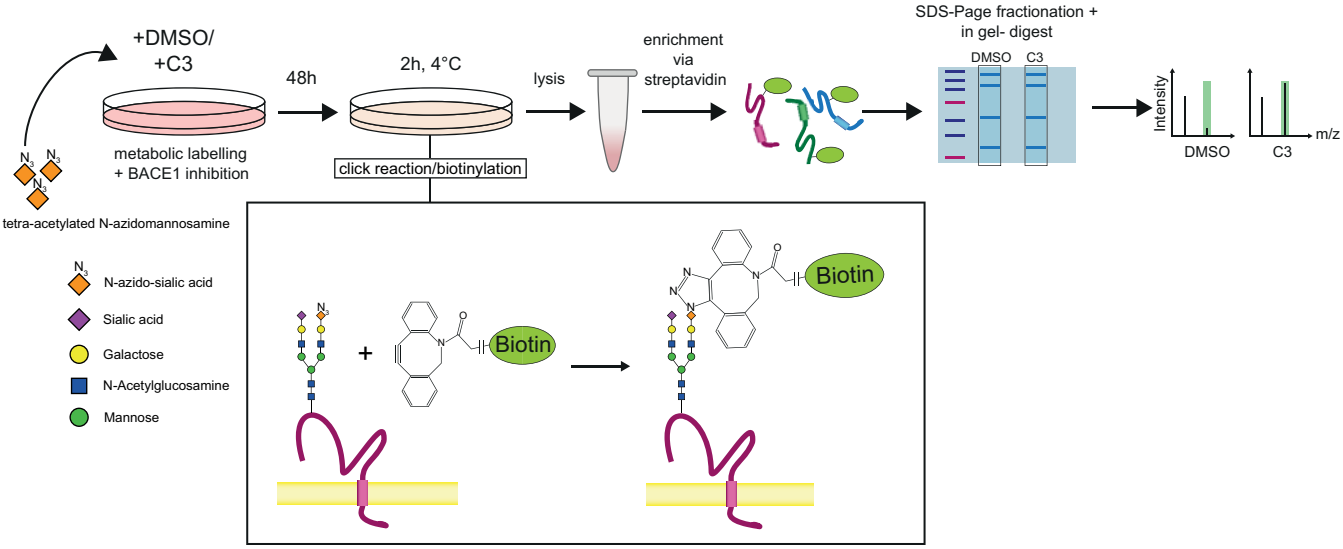

FIG. 1. **Workflow of SUSPECS method.** Cell culture medium is supplemented with tetra-acetylated N-azidoacetylmannosamine (Ac_4-ManNAz) for metabolic labeling and cells are treated with inhibitor (C3) or control (DMSO). Ac_4-ManNaz is metabolized and incorporated as modified terminal N-azido-sialic acid into glycan structures of newly synthesized proteins. After 48h cells are subjected to click mediated biotinylation for 2 h at 4 °C, during which the alkyne group of the sulfo-dibenzylcyclooctyne-biotin conjugate (DBCO) covalently reacts with the azide group of the azido-sialic acids of glycoproteins in the cell membrane (inset box). Biotinylated glycoproteins are enriched and purified with streptavidin-beads and separated via 1D-SDS-PAGE. Fractionated, in-gel digested proteins are analyzed by mass spectrometry using label-free quantification.

were washed with PBS and subsequently biotinylated with sulfo-dibenzylcyclooctyne (DBCO)-biotin on ice for two hours. In a reaction referred to as copper-free click reaction, the DBCO moiety reacts with the azido moiety of the glycoprotein, thereby leading to covalent biotinylation of the glycoprotein (Fig. 1, inset). Afterwards, cells were lysed, and the biotinylated proteins were enriched with streptavidin agarose and separated on 1D polyacrylamide gels (a representative Coomassie stained gel is shown in supplemental Fig. S2). The gel was cut into 14 fractions, subjected to in-gel tryptic digestion and analyzed by label free quantitative mass spectrometry.

To specifically label cell surface proteins, but not intracellular proteins, the sulfo-variant of DBCO-biotin was used, which carries a negative charge and should not cross the plasma membrane. To evaluate whether this is indeed true, COS7 cells were subjected to SUSPECS-mediated biotinylation. Instead of lysing cells and precipitating biotinylated proteins with streptavidin, cells were fixed and permeabilized for confocal microscopy. Biotinylated proteins were visualized with fluorescent streptavidin (streptavidin-dichlorotriazinylamino fluorescein (DTAF)) and nuclei were stained with Hoechst dye. SUSPECS-labeled cells showed a cell surface staining, with no apparent signal in the cytoplasm or intracellular organelles (Fig. 2*A* and 2*B*). As a control, cells were cultured without Ac_4-ManNAz (Fig. 2*A*, lower panel), which, as expected, did not yield a positive streptavidin-DTAF signal. This demonstrates the specificity of the fluorescent signal for biotinylated proteins as well as the selectivity of the click reaction.

Fig. 2*B* contains three confocal planes near the bottom, the middle, and the top of the streptavidin-DTAF labeled cells. The bottom plane shows contact sites of the cells to the glass coverslip, including focal adhesions and filopodia (Fig. 2*B*, arrowheads). The mid plane shows a section through the cells as they are represented in Fig. 2*A*, with a clearly distinguishable stained rim around them and the nuclei in the middle. Importantly, there was no staining of biotinylated proteins in the cytoplasm, in agreement with the specific cell surface staining. The top plane also demonstrates staining at the plasma membrane. We conclude that SUSPECS specifically labels glycosylated proteins on the cell surface.

As a further control experiment we determined biochemically whether the SUSPECS workflow indeed leads to an enrichment of cell surface proteins compared with the whole cell lysate. To this aim, cell surface proteins of primary murine neurons were biotinylated according to the SUSPECS workflow, precipitated with streptavidin, separated by gel electrophoresis and analyzed by immunoblot. Four known cell surface proteins, NEO1 (27), GluR2 (28), RGMa (29), and MT4MMP (MMP17) (30), were enriched in the surface-labeled samples (Fig. 2*C* and quantification in 2*D*). Conversely, the Golgi marker Golgin-97 (31), the ER marker calnexin (32) and the cytoskeletal protein beta actin, which do not reside at the plasma membrane, were largely depleted from the SUSPECS

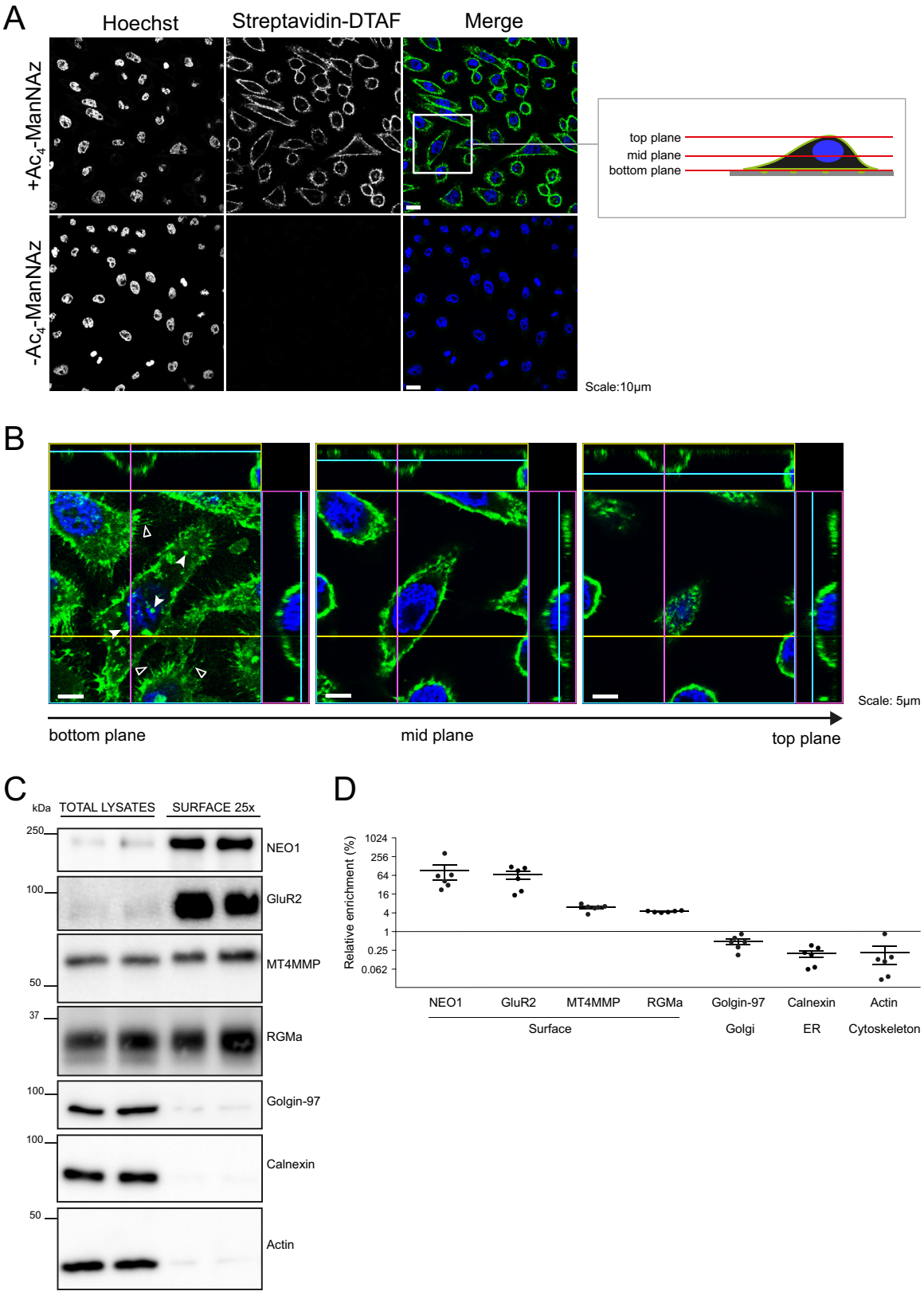

surface-labeling samples, demonstrating that SUSPECS enriches cell surface proteins (Fig. 2*C*).

SUSPECS Identifies Transmembrane Proteins at Neuronal Surface—Next, we applied SUSPECS to determine the surface glycoproteome of primary murine neurons treated with or without the BACE1 inhibitor C3. First, we generally determined the proteins at the cell surface and subsequently how their levels were changed upon BACE1 inhibition.

Proteins were considered as identified, if they were detected by at least 2 unique peptides in at least 3 out of the 12 samples (six samples each with or without C3). This yielded 3957 identified proteins (see supplemental Data S1). Although SUSPECS metabolically labels glycoproteins, the total number of proteins may also include nonglycoproteins or peripherally membrane-associated proteins, which either are bound unspecifically to the beads or are co-purified during the streptavidin pulldown as they are binding partners of glycoproteins. Thus, we focused specifically on glycosylated transmembrane and GPI-anchored proteins, which we consider as the cell surface glycoproteome in our study. Therefore, we filtered the proteins according to reviewed Uniprot annotations using the keyword "glycoprotein" as well as the subcellular location terms: single-span membrane proteins of type I, II, III or IV, as well as GPI-anchored and multipass membrane proteins. Our criteria yielded 691 transmembrane and GPI-anchored glycoproteins at the neuronal surface, with the majority being single-span type I membrane proteins (40%) or multipass membrane proteins (45%). 5 proteins had double annotations and are therefore separated into new categories (TM1/GPI, TM1/TM2, and TM1/Multi pass) (Fig. 3*A*, see supplemental Data S1 for a complete list of identified proteins). The identified unique tryptic peptides were matched to the sequence of the 691 membrane proteins using the QARIP webserver (33). As expected, the peptides were derived from the extra- and intracellular protein domains (for selected examples, see supplemental Fig. S3), but generally not from the transmembrane domains, which contain long stretches of mostly hydrophobic amino acids, but rarely a tryptic cleavage site. Only for 20 multipass proteins some peptides also contained amino acids originating from a possible transmembrane region. However, for those proteins the Uniprot transmembrane annotations were incomplete. Interestingly, for three known BACE1 substrates (CHL1, L1CAM, APLP1) we also identified peptides spanning the previously identified BACE1 cleavage sites (9, 15, 34), which are located close to the transmembrane domain (supplemental Fig. S3).

Next, we functionally categorized the transmembrane proteins according to Gene Ontology classifications using PANTHER (35). The identified transmembrane glycoproteins fell into five main functional categories (Fig. 3*B*), namely transporters (18.20%), receptors (17.57%), hydrolases (16.11%), transferases (8.79%), and signaling molecules (6.07%). Other categories (33.26%) included cell adhesion molecules, extracellular matrix proteins and defense/immunity proteins (Fig. 3*B*). Many of the identified proteins are known to be located at the neuronal cell surface according to Uniprot, which validates SUSPECS as a method for investigating the cell surface proteome. Taken together, these results demonstrate that SUSPECS identified nearly 700 neuronal surface transmembrane glycoproteins with a broad range of physiological functions, making the method applicable to various studies in the life sciences investigating cell surface proteins.

BACE Activity Modulates the Protein Composition of Neuronal Surface Membranes—Inhibition of BACE1 increases neuronal surface levels of some of its substrates, including SEZ6, SEZ6L, and CNTN-2, which led to the hypothesis that BACE1 cleavage is a general mechanism to control the levels of its substrates at the cell surface (19, 36). However, this hypothesis has not yet been tested for the numerous additional BACE1 substrates. Moreover, BACE1, which has an acidic pH optimum, does not cleave its substrates at the cell surface, but in the endosomes and the trans-Golgi network (14, 37), thus questioning whether BACE1 can generally control surface levels of all its substrates.

To resolve this open issue, we used SUSPECS and determined how pharmacological BACE1 inhibition with the established inhibitor C3 (38) affects the neuronal surface proteome. Although C3 also blocks the BACE1-homolog BACE2, we

FIG. 2. **SUSPECS labels cell surface membrane proteins.** COS7 cells were cultured with and without Ac_4-ManNAz, as indicated, and subjected to click chemistry mediated biotinylation with sulfo-DBCO. Biotinylated glycoproteins were detected with fluorescein-conjugated streptavidin (streptavidin-DTAF, green) and nuclei were stained with Hoechst dye (blue). *A*, Cells cultured in presence of Ac_4-ManNAz showed a clear streptavidin-DTAF signal on the cell surface, whereas no fluorescent signal could be detected in the cytoplasm or internal structures of the cells (upper panel). When no Ac_4-ManNAz was present, streptavidin-DTAF staining did not yield a signal (lower panel). Scale bar: 10 μm. Inset: Schematic representation of three confocal planes shown in Fig. 2*B* with a higher magnification. *B*, In the bottom plane streptavidin-DTAF signal (green) visualizes contact sites of the cells to the glass coverslip, including focal adhesions (filled arrowheads) and filopodia (clear arrowheads). The mid plane shows the cells as in Fig. 2*A*. A clear streptavidin-positive rim around the cells represents the biotinylated proteins located at the cell surface. Hoechst-stained nuclei are shown in blue. No streptavidin-signal was detected in the cytoplasm. The top plane also demonstrates staining at the plasma membrane. Scale bar: 5 μm. *C*, Primary neurons were labeled using the SUSPECS method and surface proteins were enriched by streptavidin pulldown from 25 times (25X) the volume compared with the volume loaded for the total lysate. Total neuronal lysates and SUSPECS-enriched proteins (surface) were subjected to immunoblotting for subcellular markers. NEO1, GluR2, MT4-MMP, RGMa are cell surface proteins and were enriched. Golgin-97 (Golgi marker), calnexin (ER marker) and actin (cytoskeletal protein) are not located at the cell surface and were depleted in the SUSPECS-labeled surface samples. *D*, Quantification of results in *C*. Shown are ratios of the intensities at the surface divided by the intensities in the total lysates (corrected by the factor 25 accounting for the different volumes). Ratios are expressed in percentage compared with the lysates. Given are means ± S.E.M. of $n = 6$ experiments.

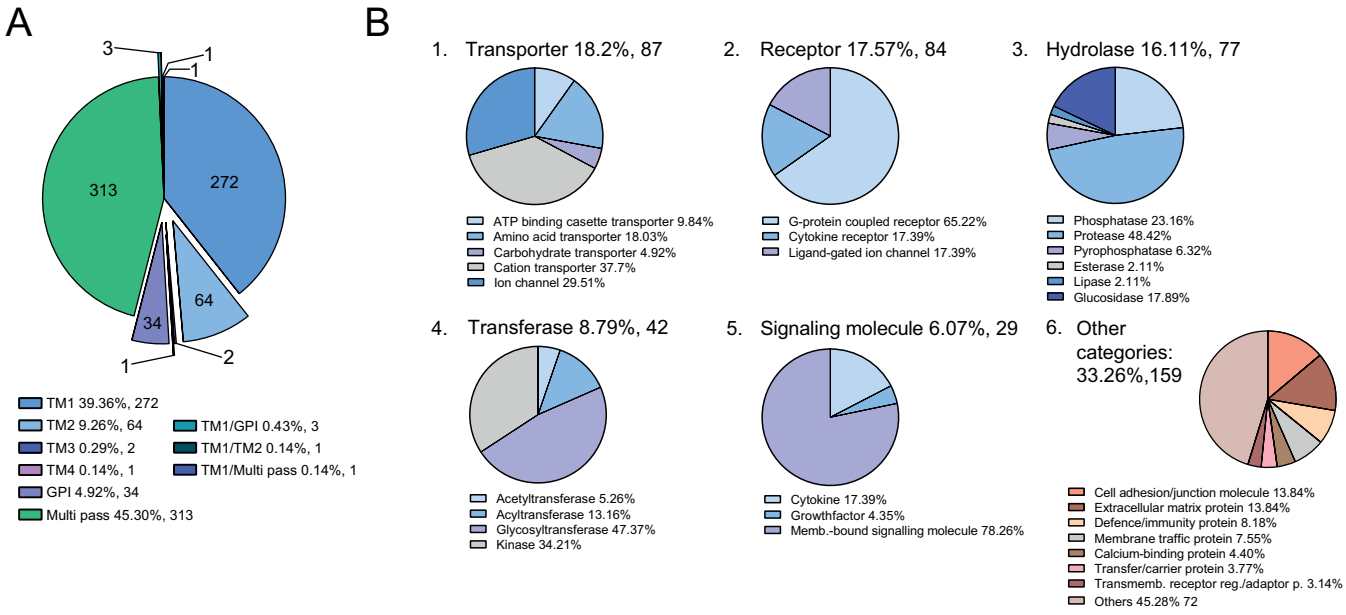

FIG. 3. **Topology and protein classification of identified transmembrane glycoproteins.** *A*, Glycosylated transmembrane proteins (691) identified with minimum 2 unique peptides in at least 3 measurements were classified using Uniprot 'subcellular locations': shown are single-pass type I membrane proteins (TM1), single-pass type II membrane proteins (TM2), single-pass type III membrane proteins (TM3), single-pass type IV membrane proteins (TM4), GPI-anchored (GPI) and multipass membrane proteins (Multi pass). *B*, Classification of identified proteins was done using the PANTHER (protein annotation through evolutionary relationship) classification system. Total number of proteins in each class is given and their percentage relative to all classified proteins that were functionally annotated in PANTHER. Note that individual proteins may fall into multiple functional classes in PANTHER. Sub-categorization of the 5 main protein classes as well as an overview of the remaining, other categories is shown as pie charts under each class. Relative percentages of functional classes in each category are given below the pie charts.

assume that changes in the surface proteome are because of BACE1 inhibition, because BACE1, but not BACE2, is highly expressed in neurons (14, 39). Overall, 471 transmembrane glycoproteins were consistently relatively quantified in at least three biological replicates, subjected to statistical evaluation, and are displayed in a volcano plot (Fig. 4). BACE1 substrates, which comprise mostly single-span and GPI-anchored proteins, were expected to show increased or unaltered protein levels upon BACE1 inhibition, whereas altered abundance of nonsubstrates would point toward secondary effects of BACE1 inhibition. Benjamini-Hochberg correction was applied to correct for multiple hypothesis using a 5% false discovery rate (FDR) (40) which resulted in $q = 0.0022$ (Fig. 4). Overall, 16 single-span transmembrane proteins (including GPI-anchored) remained significantly increased upon BACE1 inhibition after multiple hypothesis testing (Table I). Additionally, three multipass membrane proteins (LMBRD1, TSPAN6, TTYH3) were enriched and two multipass membrane proteins (SCL38A3, UBAC2) had decreased levels upon BACE1 inhibition after FDR correction.

The significantly enriched proteins can be grouped into three different categories: mildly increased (<1.5-fold), moderately increased (1.5 < fold-change < 2), and strongly increased (>2-fold). Nine proteins showed a mild increase (<1.5-fold), three multispan membrane proteins a moderate increase (>1.5 fold, but < 2-fold) and seven proteins had a strong increase (>2-fold, up to 7-fold) (Fig. 4). Six out of the seven proteins with the strongest increase (>2-fold) are single-span and GPI-anchored proteins and are known BACE1 substrates: APLP1, CNTN2, CHL1, SEZ6, SEZ6L1 and APP (14, 15, 18, 19, 41). SEZ6, SEZ6L, CNTN-2, APP, APLP1, and CHL1 were previously known to be enriched at the neuronal surface upon BACE1 inhibition (15, 19, 36, 42, 43). The seventh protein in this group is PLD3, a type II membrane protein, which is studied in AD research (44–46). In the group of proteins with a mild increase, one more known BACE1 substrate (L1CAM) and a BACE1 substrate candidate (TMEM132a) were detected (9, 15, 16). For L1CAM an accumulation on the membrane has not been shown so far (see supplemental Data S1 for a complete list of 471 proteins). The other single-span membrane proteins in the mild enrichment category, such as PODXL2 and CADM2, may be additional BACE1 substrates or be enriched as a secondary consequence of BACE1 inhibition. Taken together, the identification of known BACE1 substrates among the enriched proteins demonstrates that BACE1 can control surface levels of its substrates beyond the previously investigated proteins. Yet, the list of 471 quantified transmembrane proteins also contains several other BACE1 substrates or substrate candidates, which did not show FDR-significant changes of their surface levels. This includes DNER, SEZ6L2, GLG1, LRRN1, and NTM demonstrating that BACE1 does not lead to a sig-

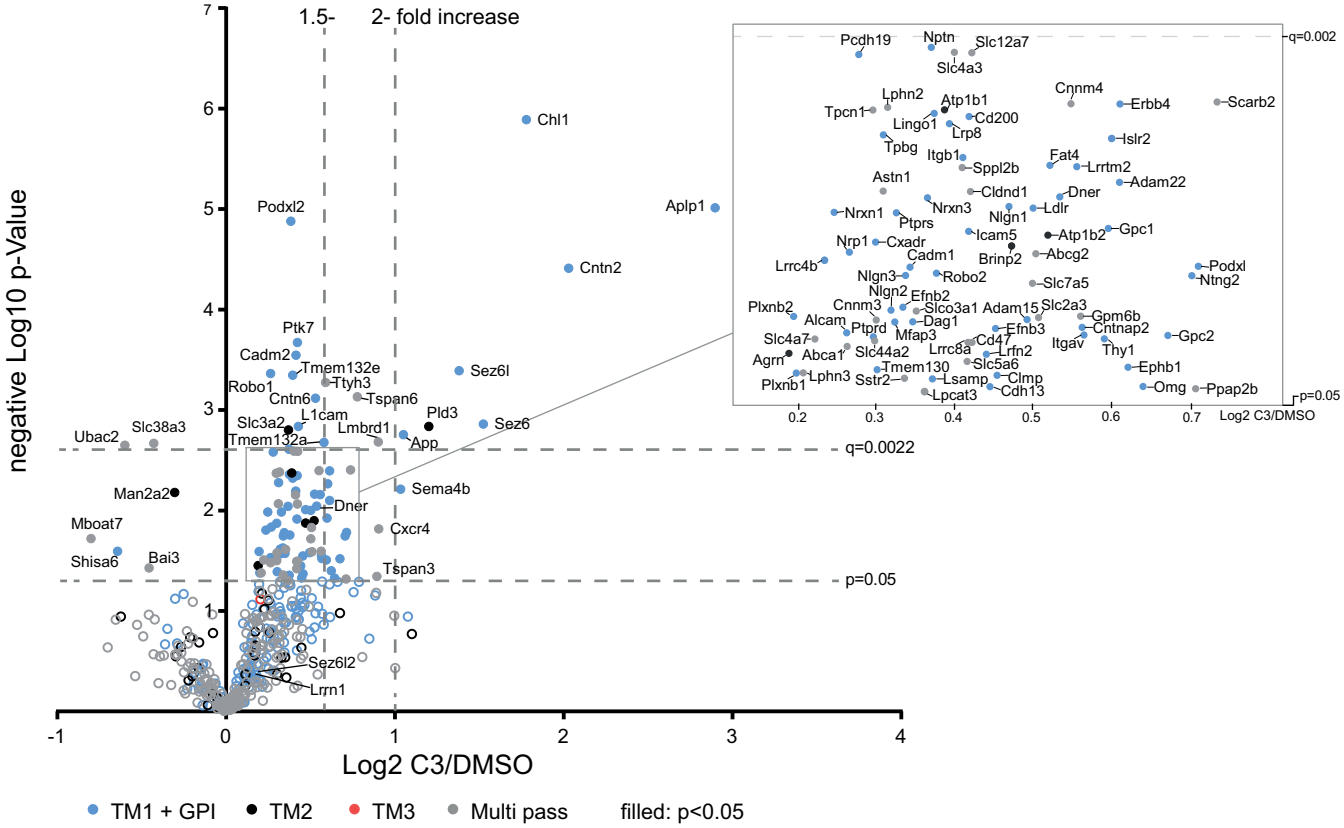

FIG. 4. **Pharmacological BACE1 inhibition selectively changes the neuronal surface glycoproteome.** Changes of glycosylated transmembrane proteins after BACE1 inhibition represented in a volcano plot. Dots and circles illustrate 471 proteins that were quantified in at least 3 biological replicates. Blue: transmembrane type I and GPI-anchored proteins (TM1+GPI), black: transmembrane type II proteins (TM2), red: transmembrane type III (TM3) proteins, and gray: multipass membrane proteins (Multi pass). The log2 fold change of BACE1 inhibition over control (Log2 C3/DMSO) is plotted against the negative log10 of each protein's *p* value according to one-sample *t* test. Filled dots represent proteins with a *p* value less than 0.05 (neg. log10 = 1.3; lower horizontal dashed line) and open circles symbolize proteins with a *p* value higher than 0.05. *Benjamini-Hochberg* correction was applied for glycosylated membrane proteins to control for false discovery rate with 5% and is marked with the higher dashed line (q = 0.0022). 106 proteins have a *p* value smaller than 0.05 and 21 proteins meet the significance criteria after false discovery rate based multiple hypothesis testing. Vertical dashed lines indicate a fold change of 1.5 and 2. Magnified box shows changes of proteins between *p* = 0.05 and q = 0.0022 up to a 2-fold increase.

nificant alteration of the surface levels of all its known substrates.

Validation of Regulated Cell Surface Proteins in Primary Neurons and BACE1-deficient Mouse Cortices—To validate the proteomic data by employing an orthogonal method, we treated primary neurons as above in an independent experiment and used immunoblots for protein detection after SUSPECS labeling and pull-down (Fig. 5). We have chosen selected BACE1 substrates that either had shown a significant increase (APLP1, SEZ6, SEZ6L), a mild, but not significant, increase (DNER) or no increase at all (SEZ6L2) in the proteomic data set. Additionally, we have chosen a presumed nonsubstrate with an increase (TSPAN6) and a known nonsubstrate MT4MMP (MMP17) (11). The increase for APLP1, SEZ6, SEZ6L and TSPAN6 observed by mass spectrometry (MS) was comparable to the significant increases seen in immunoblots (IB) (APLP1: 7.5× (MS) *versus* 7× (IB), SEZ6: 2.9× (MS) *versus* 3.6× (IB), SEZ6L: 2.6× (MS) *versus* 1.8× (IB), TSPAN6: 1.8× (MS) *versus* 3.5× (IB)) (Fig. 4 and 5*A*, 5*B*). Likewise, the unaltered abundance of SEZ6L2 and MT4MMP was validated by immunoblots. Also, for DNER the mild increase (< 1.5x) in the proteomic experiment was confirmed by immunoblot, demonstrating the reliability of the mass spectrometry-based quantification of SUSPECS labeling. Interestingly, although the mild increase of DNER levels was not significant after FDR correction in the proteomic experiment, it did reach significance in the immunoblot quantification (Fig. 5*A*, 5*B*).

From the same experiments, we also blotted the total cell lysates, which comprise the cell surface proteins, but also the intracellular proteins, including those in intracellular organelles. Protein changes in the total lysate were like the changes at the surface (Fig. 5*A*, 5*B*). SEZ6 and SEZ6L in the cell lysate displayed two protein bands in immunoblots, one carrying the immature N-glycosylation typical for a protein in the endoplasmic reticulum and Golgi (immature SEZ6 and SEZ6L) and

TABLE I

Significantly changed single-pass membrane proteins and GPI-anchored proteins. False discovery rate-corrected significant proteins are sorted by their effect size (C3/DMSO). Proteins are shown with their Uniprot accession number (Uniprot AC), their topology, change in surface levels detected upon BACE1 inhibition over control (C3/DMSO), and references in case that they were described before as BACE1 substrates

Uniprot AC	Gene name	Protein name	Topology	C3/DMSO	*p* value	References
Q03157	Aplp1	Amyloid precursor-like protein 1	Type 1	7.45	9.72E-06	(9, 15–19)
Q61330	Cntn2	Contactin-2	GPI	4.08	3.88E-05	(9, 15, 18, 19)
P70232	Chl1	Close homolog of neural cell adhesion molecule L1	Type 1	3.43	1.29E-06	(9, 15, 18, 19)
Q7TSK2	Sez6	Seizure protein 6	Type 1	2.88	1.38E-03	(9, 18, 19)
Q6P1D5	Sez6l	Seizure 6-like protein	Type 1	2.60	4.06E-04	(9, 17–19)
O35405	Pld3	Phospholipase D3	Type 2	2.30	1.45E-03	
P12023	App	Amyloid beta A4 protein (APP)	Type 1	2.07	1.76E-03	(9, 15–18)
Q922P8	Tmem132a	Transmembrane protein 132A	Type 1	1.49	2.11E-03	(9, 16)
Q9JMB8	Cntn6	Contactin-6	GPI	1.44	7.61E-04	
P11627	L1cam	Neural cell adhesion molecule L1	Type 1	1.35	1.46E-03	(9, 15, 16)
Q8BKG3	Ptk7	Inactive tyrosine-protein kinase 7	Type 1	1.34	2.13E-04	
Q8BLQ9	Cadm2	Cell adhesion molecule 2	Type 1	1.33	2.85E-04	
Q6IEE6	Tmem132e	Transmembrane protein 132E	Type 1	1.31	4.50E-04	
Q8CAE9	Podxl2	Podocalyxin-like protein 2	Type 1	1.30	1.32E-05	
P10852	Slc3a2	4F2 cell-surface antigen heavy chain	Type 2	1.29	1.57E-03	
O89026	Robo1	Roundabout homolog 1	Type 1	1.20	4.33E-04	(16)

one with a larger molecular weight carrying complex glycans (mature SEZ6 and SEZ6L) (19). At the cell surface only, the mature forms were detected (Fig. 5*A*). Interestingly, in the lysate, where both forms were detected, only the mature form but not the immature form was increased, which is consistent with BACE1 being active in post-Golgi compartments, such as trans-Golgi network and endosomes (37, 47, 48).

Given that increased protein levels were not only visible at the neuronal cell surface, but also in total neuronal lysates, we further validated the SUSPECS data *in vivo* using postnatal day 7 wild-type and BACE1-deficient mouse brain cortices. We have chosen proteins that are well detected in mouse brain by immunoblots. As cell surface labeling is not possible in brain extracts, membrane fractions containing membrane proteins and membrane-associated proteins were generated and blotted for several BACE1 substrates (APLP1, SEZ6, SEZ6L, SEZ6L2, and DNER) and for apparent nonsubstrates (TSPAN6) (Fig. 5*C*, 5*D*). Like the observations in primary neurons, levels of APLP1, SEZ6 and SEZ6L were increased in BACE1$^{-/-}$ brains, although the effect size was not as strong. In contrast to neurons, no significant change in protein level in brain cortices was observed for DNER and TSPAN6 (Fig. 5*C*, 5*D*). Unlike BACE1, which is most highly expressed in neurons, both DNER and TSPAN6 are also expressed in other brain cell types (49), where their levels may be controlled by proteases other than BACE1. This would explain increased full-length levels of both proteins specifically in neurons, but not in brain tissue upon BACE1 inactivation. SEZ6L2, which was not changed in neurons, was also not changed in the BACE1-deficient brains. Taken together, these results demonstrate that the BACE1-dependent accumulation of selected membrane proteins seen by SUSPECS was validated by immunoblots *in vitro* in primary neurons and *in vivo* in mouse brains.

BACE1 Differentially Regulates Surface and Secretome Levels of its Substrates—Using the SPECS method for secretome analysis we previously reported that different substrates are cleaved by BACE1 to different extents (9). Some substrates were only cleaved by BACE1, such that BACE1 inhibition nearly completely blocked substrate cleavage and ectodomain release into the secretome, *e.g.* for SEZ6, APLP1, L1CAM, and CHL1. However, other substrates were also cleaved by additional proteases, such as ADAM10 in the case of APP and DNER, so that BACE1 inhibition only led to a mild reduction of total ectodomain cleavage. To test whether a strong reduction in the secretome is typically coupled to a strong increase at the surface, we carried out a substrate meta-analysis comparing the effect size of surface increases obtained by SUSPECS to the secretome changes obtained previously by SPECS (Figure 6) under the same conditions, where primary neurons were treated with the BACE1 inhibitor C3 (9).

Four out of the six substrates, which showed the strongest (2–7-fold) surface increase by SUSPECS (APLP1, SEZ6, SEZ6L, CHL1), also had the most pronounced reductions in the secretome, ranging from 4–35% of cleavage remaining (Fig. 6). Conversely, DNER, SEZ6L2 and TMEM132a had a mild (<1.5-fold) or no increase of surface levels and only a mild reduction (20–40%) of their secretome levels. Thus, there is a reasonable correlation between changes at the surface and in the secretome for several substrates. Yet, a lack of correlation was observed for other substrates. APP and CNTN2 belonged to the group of substrates with strongest surface increases, but only showed a mild reduction of less than 40% in the secretome. The opposite was seen for additional substrates. For example, L1CAM, which showed a mild (1.35-fold) increase in cell surface levels, is one of the proteins with the strongest reduction in the secretome (21%

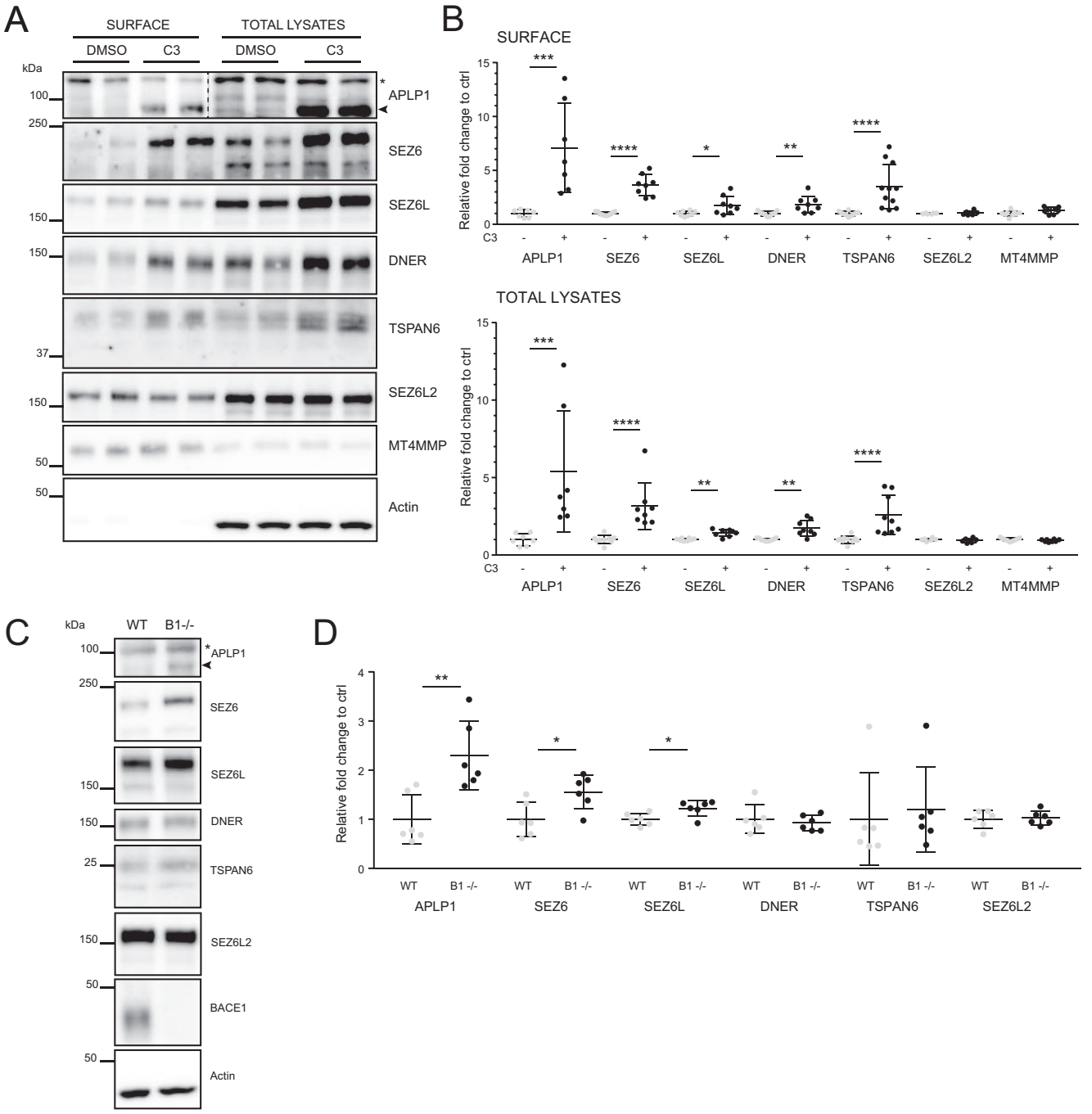

FIG. 5. **Validation of identified surface protein changes by immunoblot.** *A*, Primary neurons were treated with DMSO as control or the BACE inhibitor C3 and subjected to SUSPECS. Streptavidin-enriched glycoproteins from the surface and proteins in the total lysates were analyzed by immunoblotting. Actin was used as loading control and to evaluate the purity of the enriched surface protein fraction. No actin signal was detected in the surface fraction. Note: The vertical dashed line in the APLP1 blot indicates that the samples were run on the same gel and next to each other, but were loaded in reverse order (first total lysates then surface). For illustrative purposes, order was changed. *B*, Signals were normalized to actin levels (total lysates) or MT4MMP (surface) and ratios were quantified relative to the control condition (DMSO). APLP1, SEZ6, SEZ6L, DNER, and TSPAN6 significantly increased in total lysates (upper panel) and on the cell surface (lower panel). Statistical testing was performed with $n = 6–11$ replicates, using the Mann-Whitney-*U* test with the significance criteria of $p < 0.05$. *C*, Membrane fractions of postnatal day 7 (P7) BACE1-knockout (B1−/−) and wildtype (WT) mouse cortices were investigated by immunoblotting for protein accumulation *in vivo*. Actin- or calnexin-normalized signals were compared and quantified. Ratios are shown relative to the control (WT). APLP1, SEZ6, and SEZ6L showed significant accumulation in the membrane fraction of B1−/− cortices. DNER, TSPAN6, and SEZL2 levels did not increase significantly in B1−/− cortex membranes. Statistical testing was performed with $n = 6$ replicates, using the Mann-Whitney-*U* test with the significance criteria of $p < 0.05$. (APLP1: arrowhead = specific bands, asterisk = unspecific signals; SEZ6: m = mature, im = immature).

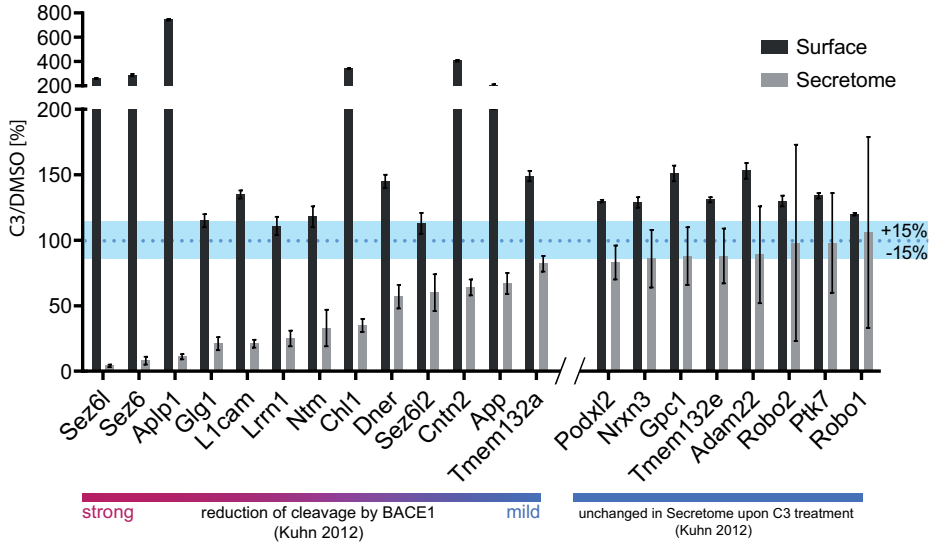

FIG. 6. **Meta-analysis of changes in surface proteome to secretome after BACE1 inhibition.** Protein level changes on the surface after BACE1 inhibition (as in Fig. 4) were compared with their changes in the secretome (according to Kuhn *et al.* 2012, (9)) for all BACE1 substrates and substrate candidates. Proteins are sorted from a strong reduction in the secretome to a mild and no change (arbitrary criteria of ± 15%, blue bar; blue dotted line indicates 100% protein level in control conditions) (light gray bars) and compared with their protein level on the surface (dark gray bars).

remaining). Likewise, GLG1, LRRN1, and NTM had their cleaved ectodomain levels reduced by more than 65%, but did not reveal a significant increase at the cell surface.

Taken together, the comparison of the SPECS and SUSPECS results reveals important insights into the molecular consequences of BACE1 inhibition in neurons. We conclude that loss of BACE1 substrate cleavage is partly coupled to corresponding substrate level increases at the neuronal surface.

DISCUSSION

Cell surface membrane proteins have a fundamental role for cell signaling in health and disease and may be proteolytically released into a cell's secretome, where they can have additional functions in cell-cell communication. Here, we demonstrate that SUSPECS is a new method for enrichment, identification, and quantification of the cell surface proteome. SUSPECS identified nearly 700 transmembrane glycoproteins at the surface of primary murine neurons and demonstrated a selective role for the protease BACE1 in remodeling the neuronal surface proteome.

SUSPECS compares well to two previously developed methods for surface protein biotinylation, cell surface capturing (CSC) and periodate oxidation and aniline-catalyzed oxime ligation (PAL). As described in more detail in the introduction, CSC and PAL use a two-step chemical labeling, where surface glycoproteins are first chemically oxidized and then labeled with a biotin-containing reagent (7, 8, 50). In contrast, SUSPECS uses a single chemical reaction based on copper-free click chemistry, which makes the method easy and fast to carry out.

In PAL and CSC sample complexity is strongly reduced by focusing on the analysis of N-glycopeptides. To this aim, PNGase F digestion is performed after tryptic digest to release the specific peptides containing the N-glycosylation site. CSC typically identified a few hundred surface glycoproteins per cell type (7), which is like the nearly 700 proteins identified here by SUSPECS. CSC was recently also used to generate a cell surface protein atlas including 1296 mouse and 1492 human cell surface glycoproteins from over 70 different cell types (51). PNGase F digestion may also be carried out after SUSPECS protein enrichment and tryptic on bead-digestion to focus on N-glycopeptides. Specific identification of the glycopeptides or biotinylated peptides has the advantage of reduced sample complexity but comes with the disadvantage that only few peptides are identified per protein and can be used for quantitative proteomics. Therefore, we have chosen to analyze all tryptic peptides in SUSPECS to achieve reliable relative label free protein quantification, which may also be feasible with CSC and PAL.

Recently, a method for enrichment and quantification of biotinylated peptides called "direct detection of biotin-containing tags" (DiDBiT) was developed, which reduces binding of nonspecific proteins to beads (52). A modified version of our protocol for cell surface labeling protocol may also be combined with DiDBiT. Because glycans and not amino acids are labeled in our SUSPECS protocol, the metabolic labeling of amino acids would have to be performed using azidohomoalanine (AHA) (13), an amino acid analog of methionine which contains an azido moiety, instead of Ac_4-ManNAz. After biotin labeling using sulfo-DBCO-biotin, DiDBiT could be employed to quantify only biotinylated peptides (52). Yet, AHA is cyto-

toxic and therefore requires a careful titration of subtoxic concentration individually for each cell type.

A limitation of all three methods (SUSPECS, CSC, PAL) is that they specifically enrich for glycosylated cell surface membrane proteins. Yet, this limitation appears acceptable for proteomic discovery experiments, given that a large fraction of membrane proteins is indeed glycosylated (supplemental Fig. S1). Moreover, compared with direct biotinylation of lysine side chains in surface proteins, *e.g.* by sulfo-NHS-biotin, the three methods SUSPECS, CSC and PAL allow tryptic digest of the biotinylated proteins which is well suited for subsequent mass spectrometric analysis.

An advantage of SUSPECS over the other cell surface proteomics methods is the possibility to combine it with SPECS for secretome analysis in the presence of serum or other protein containing cell culture medium supplements, as only newly synthesized cellular proteins are metabolically labeled with the click sugar. Serum and supplements are often required for primary cells and to keep cells under physiological conditions (13). Because of the metabolic labeling step, SUSPECS is particularly useful for cells or tissues in culture, whereas CSC and PAL may also be used with freshly prepared cells or tissues that are not taken into culture as no metabolic labeling step is required.

A comparison of surface proteome and secretome can yield new and unexpected insights into biology. This is shown in our study with the example of BACE1 inhibition, which selectively remodeled a small fraction (4%) of the quantified surface proteome (21 out of 471 proteins), including eight BACE1 substrates. This was unexpected, because under the same conditions BACE1 inhibition reduced shedding of more than 30 substrates and substrate candidates in the secretome (9). Potentially, BACE1 controls surface levels of more than the eight substrates identified here, as seen with the protein DNER. Although DNER did not show a significant increase at the cell surface in the proteomic analysis when applying strict multiple hypothesis testing corrections, we validated the mild increase of DNER surface levels by immunoblot analysis.

The selective surface accumulation of only some substrates upon BACE1 inhibition may result from different molecular mechanisms. Several of the strongly ($>$ 2-fold) accumulating BACE1 substrates (APLP1, SEZ6, SEZ6L, CHL1) are nearly exclusively cleaved by BACE1 in neurons and not by other proteases (15, 19, 41), demonstrating that in the absence of BACE1 activity no other protease compensates and consequently the full-length membrane proteins accumulate within cells and at the cell surface. Conversely, another substrate, SEZ6L2, which is only partially shed by BACE1 and mostly by other proteases (9), was not significantly increased at the cell surface. However, a correlation between the extent of BACE1 cleavage and surface accumulation was not occurring for all substrates, including CNTN-2 and APP. Both proteins are also shed by other proteases, but still accumulated at the neuronal surface upon BACE1 inhibition. The opposite was seen for L1CAM, where shedding was nearly completely inhibited, but surface levels were only mildly increased. The poor correlation seen for some substrates may result from different molecular mechanisms. For example, if only a small fraction of the substrate is shed, BACE1 inhibition may completely block shedding but only mildly increase surface levels of the substrate, as it was seen for L1CAM. Another mechanism explaining the selective surface substrate enrichment might be the cellular compartment where BACE1 cleaves its substrates. BACE1 has an acidic pH and cleaves its substrates in acidic cellular compartments, in endosomes and the trans-Golgi network (14, 37). If BACE1 cleavage is blocked, some uncleaved substrates may be transported to the cell surface and accumulate. Yet other substrates, if uncleaved, may not be transported further, but instead reside within endosomes/TGN or be degraded, and thus, not accumulate at the cell surface. As an additional mechanism it is conceivable that BACE1 substrates with a long half-life could possibly show a stronger accumulation upon BACE1 inhibition than substrates with a short half-life, as an excess of the latter ones may be rapidly degraded by other cellular mechanisms. Yet, proteins with both a long and a short half-life are well detected by SUSPECS because of the continuous labeling with the click sugar. This is for example seen with the efficient detection of APP, a protein with a known half-life of less than one hour (53, 54).

Even though only few proteins were increased at the neuronal surface upon BACE1 inhibition, this may have consequences for the function of the affected proteins, for example for CNTN-2 and APLP1. Increased surface levels of the neural adhesion molecule CNTN-2 were suggested to alter cell adhesion, neurite outgrowth and axon guidance (36), and may, thus, contribute to some of the phenotypes reported for BACE1-deficient mice (55). APLP1 acts as a transcellular adhesion molecule at the synapse (56). Altered APLP1 expression affects synapse formation *in vitro* and *in vivo* (57) such that the increased APLP1 surface levels in BACE1-inhibited and BACE1-deficient conditions may interfere with synapse formation and maintenance, which are known to be altered in BACE1-deficient mice (58–60). Additionally, also loss of APLP1 results in reduced spine density in aged mice (57). Not only substrates, but also apparent nonsubstrates of BACE1, such as TSPAN6, accumulated at the neuronal cell surface, suggesting that BACE1 inhibition may have more potential mechanism-based consequences than expected.

In summary, SUSPECS is a new, easy, and rapid method for determination of the cell surface glycoproteome. A major strength of the method is that—beyond surface proteome analysis—it can be combined with SPECS-based secretome analyses in the presence of serum or other media supplements within the same experiment. Although we have demonstrated the power of the approach using the example of the Alzheimer protease BACE1, other applications of combining SUSPECS with secretome studies may range from cell-secre-

tome changes under inflammatory conditions to cross-talk between different cell types and the study of other cell surface proteases, many of which have essential functions in (patho) physiological conditions.

DATA AVAILABILITY

The mass spectrometry proteomics data have been deposited to the ProteomeXchange Consortium via the PRIDE (24) partner repository with the data set identifier PXD008619. Project webpage: http://www.ebi.ac.uk/pride/archive/projects/PXD008619.

* This work was supported by the DFG (SyNergy EXC1010, FOR2290, MU1457/14-1, GRK 2039), the Israel-Helmholtz program, the Centers of Excellence in Neurodegeneration program, the Helmholtz program Biointerfaces in Technology and Medicine, and the Breuer Foundation Research Award. JN was supported by a BAYHOST fellowship.

[S] This article contains supplemental material.

¶¶ To whom correspondence should be addressed: German Center for Neurodegenerative Diseases (DZNE), Munich, Germany. Tel.: +49.89.4400.46426; Fax: +49.89.4400.46429; E-mail: Stefan.Lichtenthaler@dzne.de.

|||| Shared first authors.

Author contributions: J.H., J.N., S.A.M., and S.F.L. conceived the project and planned experiments. J.H. performed proteomic and immunofluorescence experiments and contributed to biochemical experiments; J.N. performed biochemical experiments; J.H., J.N., and S.A.M. analyzed data; R.F. and U.M. contributed to generation of the APLP1 antibody; U.S. and S.B. provided the Ac_4-ManNAz; J.H., S.A.M., and S.F.L. wrote the manuscript with input from all authors.

REFERENCES

1. Yildirim, M. A., Goh, K. I., Cusick, M. E., Barabasi, A. L., and Vidal, M. (2007) Drug-target network. *Nat. Biotechnol.* **25,** 1119–1126
2. Saftig, P., and Lichtenthaler, S. F. (2015) The alpha secretase ADAM10: A metalloprotease with multiple functions in the brain. *Prog. Neurobiol.* **135,** 1–20
3. Yan, R. (2017) Physiological functions of the beta-site amyloid precursor protein cleaving enzyme 1 and 2. *Front. Mol. Neurosci.* **10,** 97
4. Zunke, F., and Rose-John, S. (2017) The shedding protease ADAM17: Physiology and pathophysiology. *Biochim. Biophys. Acta* **1864,** 2059–2070
5. McCarthy, A. J., Coleman-Vaughan, C., and McCarthy, J. V. (2017) Regulated intramembrane proteolysis: emergent role in cell signalling pathways. *Biochem. Soc. Trans.* **45,** 1185–1202
6. Wisniewski, J. R. (2011) Tools for phospho- and glycoproteomics of plasma membranes. *Amino Acids* **41,** 223–233
7. Wollscheid, B., Bausch-Fluck, D., Henderson, C., O'Brien, R., Bibel, M., Schiess, R., Aebersold, R., and Watts, J. D. (2009) Mass-spectrometric identification and relative quantification of N-linked cell surface glycoproteins. *Nat. Biotechnol.* **27,** 378–386
8. Zeng, Y., Ramya, T. N., Dirksen, A., Dawson, P. E., and Paulson, J. C. (2009) High-efficiency labeling of sialylated glycoproteins on living cells. *Nat. Methods* **6,** 207–209
9. Kuhn, P. H., Koroniak, K., Hogl, S., Colombo, A., Zeitschel, U., Willem, M., Volbracht, C., Schepers, U., Imhof, A., Hoffmeister, A., Haass, C., Rossner, S., Brase, S., and Lichtenthaler, S. F. (2012) Secretome protein enrichment identifies physiological BACE1 protease substrates in neurons. *EMBO J.* **31,** 3157–3168
10. Kuhn, P., Voss, M., Haug-Kröper, M., Schröder, B., Schepers, U., Bräse, S., Haass, C., Lichtenthaler, S., and Fluhrer, R. (2015) Secretome analysis identifies novel signal Peptide peptidase-like 3 (Sppl3) substrates and reveals a role of Sppl3 in multiple Golgi glycosylation pathways. *Mol. Cell. Protomics* **14,** 1584–1598
11. Kuhn, P. H., Colombo, A. V., Schusser, B., Dreymueller, D., Wetzel, S., Schepers, U., Herber, J., Ludwig, A., Kremmer, E., Montag, D., Muller, U., Schweizer, M., Saftig, P., Brase, S., and Lichtenthaler, S. F. (2016) Systematic substrate identification indicates a central role for the metalloprotease ADAM10 in axon targeting and synapse function. *Elife* **5**
12. Serdaroglu, A., Muller, S. A., Schepers, U., Brase, S., Weichert, W., Lichtenthaler, S. F., and Kuhn, P. H. (2017) An optimised version of the secretome protein enrichment with click sugars (SPECS) method leads to enhanced coverage of the secretome. *Proteomics* **17**
13. Eichelbaum, K., Winter, M., Berriel Diaz, M., Herzig, S., and Krijgsveld, J. (2012) Selective enrichment of newly synthesized proteins for quantitative secretome analysis. *Nat. Biotechnol.* **30,** 984–990
14. Vassar, R. (1999) Beta-secretase cleavage of Alzheimer's amyloid precursor protein by the transmembrane aspartic protease BACE. *Science* **286,** 735–741
15. Zhou, L., Barao, S., Laga, M., Bockstael, K., Borgers, M., Gijsen, H., Annaert, W., Moechars, D., Mercken, M., Gevaert, K., and De Strooper, B. (2012) The neural cell adhesion molecules L1 and CHL1 are cleaved by BACE1 protease in vivo. *J. Biol. Chem.* **287,** 25927–25940
16. Hemming, M. L., Elias, J. E., Gygi, S. P., and Selkoe, D. J. (2009) Identification of beta-secretase (BACE1) substrates using quantitative proteomics. *PLoS ONE* **4,** e8477
17. Stutzer, I., Selevsek, N., Esterhazy, D., Schmidt, A., Aebersold, R., and Stoffel, M. (2013) Systematic proteomic analysis identifies beta-site amyloid precursor protein cleaving enzyme 2 and 1 (BACE2 and BACE1) substrates in pancreatic beta-cells. *J. Biol. Chem.* **288,** 10536–10547
18. Dislich, B., Wohlrab, F., Bachhuber, T., Muller, S. A., Kuhn, P. H., Hogl, S., Meyer-Luehmann, M., and Lichtenthaler, S. F. (2015) Label-free quantitative proteomics of mouse cerebrospinal fluid detects beta-site APP cleaving enzyme (BACE1) protease substrates in vivo. *Mol. Cell. Proteomics* **14,** 2550–2563
19. Pigoni, M., Wanngren, J., Kuhn, P. H., Munro, K. M., Gunnersen, J. M., Takeshima, H., Feederle, R., Voytyuk, I., De Strooper, B., Levasseur, M. D., Hrupka, B. J., Muller, S. A., and Lichtenthaler, S. F. (2016) Seizure protein 6 and its homolog seizure 6-like protein are physiological substrates of BACE1 in neurons. *Mol. Neurodegener.* **11,** 67
20. Vassar, R., Kuhn, P. H., Haass, C., Kennedy, M. E., Rajendran, L., Wong, P. C., and Lichtenthaler, S. F. (2014) Function, therapeutic potential and cell biology of BACE proteases: current status and future prospects. *J. Neurochem.* **130,** 4–28
21. Köhler, G., and Milstein, C. (1975) Continuous cultures of fused cells secreting antibody of predefined specificity. *Nature* **256,** 495–497
22. Colombo, A., Wang, H., Kuhn, P. H., Page, R., Kremmer, E., Dempsey, P. J., Crawford, H. C., and Lichtenthaler, S. F. (2013) Constitutive alpha- and beta-secretase cleavages of the amyloid precursor protein are partially coupled in neurons, but not in frequently used cell lines. *Neurobiol. Dis.* **49,** 137–147
23. Shevchenko, A., Tomas, H., Havlis, J., Olsen, J. V., and Mann, M. (2006) In-gel digestion for mass spectrometric characterization of proteins and proteomes. *Nat. Protoc.* **1,** 2856–2860
24. Vizcaino, J. A., Csordas, A., del-Toro, N., Dianes, J. A., Griss, J., Lavidas, I., Mayer, G., Perez-Riverol, Y., Reisinger, F., Ternent, T., Xu, Q. W., Wang, R., and Hermjakob, H. (2016) 2016 update of the PRIDE database and its related tools. *Nucleic Acids Res.* **44,** D447–D456
25. Laughlin, S. T., and Bertozzi, C. R. (2007) Metabolic labeling of glycans with azido sugars and subsequent glycan-profiling and visualization via Staudinger ligation. *Nat. Protoc.* **2,** 2930–2944
26. Mende, M., Bednarek, C., Wawryszyn, M., Sauter, P., Biskup, M. B., Schepers, U., and Brase, S. (2016) Chemical synthesis of glycosaminoglycans. *Chem. Rev.* **116,** 8193–8255
27. Vielmetter, J. (1994) Neogenin, an avian cell surface protein expressed during terminal neuronal differentiation, is closely related to the human tumor suppressor molecule deleted in colorectal cancer. *J. Cell Biol.* **127,** 2009–2020
28. Martin, L. J., Blackstone, C. D., Levey, A. I., Huganir, R. L., and Price, D. L. (1993) AMPA glutamate receptor subunits are differentially distributed in rat brain. *Neuroscience* **53,** 327–358
29. Niederkofler, V., Salie, R., Sigrist, M., and Arber, S. (2004) Repulsive guidance molecule (RGM) gene function is required for neural tube closure

but not retinal topography in the mouse visual system. *J. Neurosci.* **24,** 808–818
30. Itoh, Y., Kajita, M., Kinoh, H., Mori, H., Okada, A., and Seiki, M. (1999) Membrane Type 4 Matrix Metalloproteinase (MT4-MMP, MMP-17) Is a Glycosylphosphatidylinositol-anchored Proteinase. *J. Biol. Chem.* **274,** 34260–34266
31. Griffith, K. J., Chan, E. K., Lung, C. C., Hamel, J. C., Guo, X., Miyachi, K., and Fritzler, M. J. (1997) Molecular cloning of a novel 97-kd Golgi complex autoantigen associated with Sjogren's syndrome. *Arthritis Rheumatism* **40,** 1693–1702
32. Wada, I., Rindress, D., Cameron, P. H., Ou, W. J., Doherty, J. J., Louvard, D., Bell, A. W., Dignard, D., Thomas, D. Y., and Bergeron, J. J. (1991) SSR alpha and associated calnexin are major calcium binding proteins of the endoplasmic reticulum membrane. *J. Biochem.* **266,** 19599–19610
33. Ivankov, D. N., Bogatyreva, N. S., Honigschmid, P., Dislich, B., Hogl, S., Kuhn, P. H., Frishman, D., and Lichtenthaler, S. F. (2013) QARIP: a web server for quantitative proteomic analysis of regulated intramembrane proteolysis. *Nucleic Acids Res.* **41,** W459–W464
34. Yanagida, K., Okochi, M., Tagami, S., Nakayama, T., Kodama, T. S., Nishitomi, K., Jiang, J., Mori, K., Tatsumi, S., Arai, T., Ikeuchi, T., Kasuga, K., Tokuda, T., Kondo, M., Ikeda, M., Deguchi, K., Kazui, H., Tanaka, T., Morihara, T., Hashimoto, R., Kudo, T., Steiner, H., Haass, C., Tsuchiya, K., Akiyama, H., Kuwano, R., and Takeda, M. (2009) The 28-amino acid form of an APLP1-derived Abeta-like peptide is a surrogate marker for Abeta42 production in the central nervous system. *EMBO Mol. Med.* **1,** 223–235
35. Mi, H., Muruganujan, A., Casagrande, J. T., and Thomas, P. D. (2013) Large-scale gene function analysis with the PANTHER classification system. *Nat. Protoc.* **8,** 1551–1566
36. Gautam, V., D'Avanzo, C., Hebisch, M., Kovacs, D. M., and Kim, D. Y. (2014) BACE1 activity regulates cell surface contactin-2 levels. *Mol. Neurodegeneration*
37. Hook, V., Toneff, T., Aaron, W., Yasothornsrikul, S., Bundey, R., and Reisine, T. (2002) Beta-amyloid peptide in regulated secretory vesicles of chromaffin cells: evidence for multiple cysteine proteolytic activities in distinct pathways for beta-secretase activity in chromaffin vesicles. *J. Neurochem.* **81,** 237–256
38. Stachel, S. J., Coburn, C. A., Steele, T. G., Jones, K. G., Loutzenhiser, E. F., Gregro, A. R., Rajapakse, H. A., Lai, M. T., Crouthamel, M. C., Xu, M., Tugusheva, K., Lineberger, J. E., Pietrak, B. L., Espeseth, A. S., Shi, X. P., Chen-Dodson, E., Holloway, M. K., Munshi, S., Simon, A. J., Kuo, L., and Vacca, J. P. (2004) Structure-based design of potent and selective cell-permeable inhibitors of human beta-secretase (BACE-1). *J. Med. Chem.* **47,** 6447–6450
39. Bennett, B. D., Babu-Khan, S., Loeloff, R., Louis, J. C., Curran, E., Citron, M., and Vassar, R. (2000) Expression analysis of BACE2 in brain and peripheral tissues. *J. Biol. Chem.* **275,** 20647–20651
40. Diz, A. C.-R., A; Skibinski, D. O. (2011) Multiple hypothesis testing in proteomics: a strategy for experimental work. *Mol. Cell. Protomics* **10**
41. Li, Q., and Sudhof, T. C. (2004) Cleavage of amyloid-beta precursor protein and amyloid-beta precursor-like protein by BACE 1. *J. Biol. Chem.* **279,** 10542–10550
42. Nigam, S. M., Xu, S., Ackermann, F., Gregory, J. A., Lundkvist, J., Lendahl, U., and Brodin, L. (2016) Endogenous APP accumulates in synapses after BACE1 inhibition. *Neurosci. Res.* **109,** 9–15
43. Frigerio, C., Fadeeva, J. V., Minogue, A. M., Citron, M., Van Leuven, F., Staufenbiel, M., Paganetti, P., Selkoe, D. J., and Walsh, D. M. (2010) beta-Secretase cleavage is not required for generation of the intracellular C-terminal domain of the amyloid precursor family of proteins. *FEBS J.* **277,** 1503–1518
44. Cruchaga, C., Karch, C. M., Jin, S. C., Benitez, B. A., Cai, Y., Guerreiro, R., Harari, O., Norton, J., Budde, J., Bertelsen, S., Jeng, A. T., Cooper, B., Skorupa, T., Carrell, D., Levitch, D., Hsu, S., Choi, J., Ryten, M., Sassi, C., Bras, J., Gibbs, R. J., Hernandez, D. G., Lupton, M. K., Powell, J., Forabosco, P., Ridge, P. G., Corcoran, C. D., Tschanz, J. T., Norton, M. C., Munger, R. G., Schmutz, C., Leary, M., Demirci, F. Y., Bamne, M. N., Wang, X., Lopez, O. L., Ganguli, M., Medway, C., Turton, J., Lord, J., Braae, A., Barber, I., Brown, K., Alzheimer's Research, U. K. C., Pastor, P., Lorenzo-Betancor, O., Brkanac, Z., Scott, E., Topol, E., Morgan, K., Rogaeva, E., Singleton, A., Hardy, J., Kamboh, M. I., George-Hyslop, P. S., Cairns, N., Morris, J. C., Kauwe, J. S. K., and Goate, A. M. (2014) Rare coding variants in the phospholipase D3 gene confer risk for Alzheimer's disease. *Nature* **505,** 550–554
45. Satoh, J., Kino, Y., Yamamoto, Y., Kawana, N., Ishida, T., Saito, Y., and Arima, K. (2014) PLD3 is acumulated on neuritic plaques in Alzheimer's disease brains. *Alzheimer's Res. Therapy*
46. Fazzari, P., Horre, K., Arranz, A. M., Frigerio, C. S., Saito, T., Saido, T. C., and De Strooper, B. (2017) PLD3 gene and processing of APP. *Nature* **541,** E1–E2
47. Huse, J. T., Pijak, D. S., Leslie, G. J., Lee, V. M., and Doms, R. W. (2000) Maturation and endosomal targeting of beta-site amyloid precursor protein-cleaving enzyme. The Alzheimer's disease beta-secretase. *J. Biol. Chem.* **275,** 33729–33737
48. Pastorino, L., Ikin, A. F., Nairn, A. C., Pursnani, A., and Buxbaum, J. D. (2002) The carboxyl-terminus of BACE contains a sorting signal that regulates BACE trafficking but not the formation of total A(beta). *Mol. Cell. Neurosci.* **19,** 175–185
49. Sharma, K., Schmitt, S., Bergner, C. G., Tyanova, S., Kannaiyan, N., Manrique-Hoyos, N., Kongi, K., Cantuti, L., Hanisch, U. K., Philips, M. A., Rossner, M. J., Mann, M., and Simons, M. (2015) Cell type- and brain region-resolved mouse brain proteome. *Nat. Neurosci.* **18,** 1819–1831
50. Ramya, T. N., Weerapana, E., Cravatt, B. F., and Paulson, J. C. (2013) Glycoproteomics enabled by tagging sialic acid- or galactose-terminated glycans. *Glycobiology* **23,** 211–221
51. Bausch-Fluck, D., Hofmann, A., Bock, T., Frei, A. P., Cerciello, F., Jacobs, A., Moest, H., Omasits, U., Gundry, R. L., Yoon, C., Schiess, R., Schmidt, A., Mirkowska, P., Hartlova, A., Van Eyk, J. E., Bourquin, J. P., Aebersold, R., Boheler, K. R., Zandstra, P., and Wollscheid, B. (2015) A mass spectrometric-derived cell surface protein atlas. *PLoS ONE* **10,** e0121314
52. Schiapparelli, L. M., McClatchy, D. B., Liu, H. H., Sharma, P., JRYates 3rd, Cline, H. T. (2014) Direct detection of biotinylated proteins by mass spectrometry. *J. Proteome Res.* **13,** 3966–3978
53. Gersbacher, M. T., Goodger, Z. V., Trutzel, A., Bundschuh, D., Nitsch, R. M., and Konietzko, U. (2013) Turnover of amyloid precursor protein family members determines their nuclear signaling capability. *PLoS ONE* **8,** e69363
54. Weidemann, A., Bunke, G. K. D., Fischer, P., Salbaum, J. M., Masters, C. L., and Beyreuther, K. (1989) Identification, biogenesis, and localization of precursors of Alzheimer's disease A4 amyloid protein. *Cell* **57,** 115–126
55. Vassar, R. (2014) BACE1 inhibitor drugs in clinical trials for Alzheimer's disease. *Alzheimer's Res. Therapy*
56. Muller, U. C., Deller, T., and Korte, M. (2017) Not just amyloid: physiological functions of the amyloid precursor protein family. *Nat. Rev. Neurosci.* **18,** 281–298
57. Schilling, S., Mehr, A., Ludewig, S., Stephan, J., Zimmermann, M., August, A., Strecker, P., Korte, M., Koo, E. H., Muller, U. C., Kins, S., and Eggert, S. (2017) APLP1 Is a Synaptic Cell Adhesion Molecule, Supporting Maintenance of Dendritic Spines and Basal Synaptic Transmission. *J. Neurosci.* **37,** 5345–5365
58. Zhu, K., Xiang, X., Filser, S., Marinkovic, P., Dorostkar, M. M., Crux, S., Neumann, U., Shimshek, D. R., Rammes, G., Haass, C., Lichtenthaler, S. F., Gunnersen, J. M., and Herms, J. (2016) Beta-Site Amyloid Precursor Protein Cleaving Enzyme 1 Inhibition Impairs Synaptic Plasticity via Seizure Protein 6. *Biol. Psychiatry,* **83,** 428–437
59. Filser, S., Ovsepian, S. V., Masana, M., Blazquez-Llorca, L., Brandt Elvang, A., Volbracht, C., Muller, M. B., Jung, C. K., and Herms, J. (2015) Pharmacological inhibition of BACE1 impairs synaptic plasticity and cognitive functions. *Biol. Psychiatry* **77,** 729–739
60. Savonenko, A. V., Melnikova, T., Laird, F. M., Stewart, K. A., Price, D. L., and Wong, P. C. (2008) Alteration of BACE1-dependent NRG1/ErbB4 signaling and schizophrenia-like phenotypes in BACE1-null mice. *Proc. Natl. Acad. Sci. U.S.A.* **105,** 5585–5590